



ORIGINAL RESEARCH PAPER

Radio-Diagnosis

STUDY OF MESENTERIC LYMPH NODE EVALUATION- ULTRASOUND, SURGICAL & PATHOLOGICAL CORRELATION

KEY WORDS:

Dr. Vimal Dugad	Resident, Department of Radiology, MGM medical college, Aurangabad
Dr R J Totla	MS, MCH, Paed. Surgeon, Asso. Prof MGM Medical college, Aurangabad, TotlaHosp, Aurangabad.
Dr P S Mishrikotkar	MD, Rad. Prof of Radiology MGM medical College, Aurangabad & Shanti Imaging Centre, Aurangabad
Dr. Sayali Umale	Resident, Department of Radiology, MGM medical college, Aurangabad
Dr. Srushti Bajaj	Resident, Department of Radiology, MGM medical college, Aurangabad
Dr. Shreya Sashi	Resident, Department of Radiology, MGM medical college, Aurangabad

ABSTRACT

Background: Enlarged mesenteric lymph nodes (MLN) are frequently seen in children with abdominal pain. Mesenteric lymphadenitis is a common clinical finding in the pediatric population. Mesenteric lymphadenitis in childhood is known to have varied clinical presentations & that include fever and abdominal pain, inflammations, infections, malignancy, lymphoma etc. Physical examination has limited role. Imaging studies like ultrasound help in making the diagnosis. Because abdominal ultrasonography (US) does not expose the child to radiation, it is often the primary imaging choice in clinical practice. Color Doppler flow imaging (CDFI) is a non-invasive technique to investigate the cause of abdominal pain in pediatric patients. When in doubt needs surgico-pathological correlation.

INTRODUCTION

Conventional ultrasound (US) is the recommended imaging method for lymph node (LN) diseases with the advantages of high-resolution, real-time evaluation and relative low costs, also helps in the guidance for LN biopsy. Recent advances in US technology, such as contrast enhanced ultrasound (CEUS), contrast enhanced endoscopic ultrasound (CE-EUS), and real time elastography show potential to improve the accuracy of US for the differential diagnosis of benign and malignant lymph nodes. In addition, CEUS and CE-EUS have been also used for the guidance of fine needle aspiration and assessment of treatment response. Complementary to size criteria, CEUS could also be used to evaluate response of tumor angiogenesis to anti-angiogenic therapies. In this paper we review current literature regarding evaluation of lymphadenopathy by new and innovative US techniques

OBJECTIVE

To evaluate the prevalence of enlarged MLN (short axis ≥5 mm) as detected by abdominal Ultrasound, wherever needed CT, surgical correlation & their histopathological confirmation in children with a low likelihood for mesenteric lymphadenopathy

MATERIAL AND METHODS

During a 23-month period from Jan 2019 to Dec 2020 at MGM medical college hospital & Totla hospital were identified. All patients undergone ultrasound examination. Wherever needed, contrast enhanced abdominal CT examinations performed for evaluation of mesenteric adenitis & those who needed surgery were compared with Ultrasound diagnosis. Enlarged mesenteric nodes measured in short-axis diameter and noted the quadrant location. The nodes were characterized on ultrasound & color doppler appearance being acutely inflamed, chronic adenitis, tuberculous, malignant etc & followed up on ultrasound, where needed surgical excision or ultrasound guided biopsy for confirmation. Mesenteric lymphadenitis is a common clinical finding in the pediatric population. Mesenteric lymphadenitis in childhood is known to have varied clinical presentations that can include fever and abdominal pain. However, physical examination alone is often limited in the young child and requires imaging studies to make the diagnosis. Because abdominal ultrasonography (US) does not expose the child to radiation, it is often the primary imaging

choice in clinical practice [1]. Color Doppler flow imaging (CDFI) is a non-invasive technique to investigate the cause of abdominal pain in pediatric patients [2]. All lymph nodes in the study group and the control group underwent grayscale ultrasound (US), color Doppler flow imaging (CDFI), and superb microvascular imaging (SMI) imaging. All the ultrasound examinations were conducted using a Philips Epiq 7G or Samsung Hera W 10 ultrasound, GE voluson E8 system with 12 to 18 MHz line array transducer. All patients in both groups first underwent US examination with transverse and longitudinal scans of the lower abdomen. Conventional ultrasonic characteristics including size, shape, and echogenicity were recorded for further analysis. The number of lymph nodes, their localizations, dimensions, shape, and architecture were recorded. Size referred to the longest (L) axis and shortest (S) axis, while shape referred to the ratio of L to S axis (L/S). CDFI (frame rate, 10–15 Hz) and SMI (frame rate, >50 Hz) were used to assess vascular imaging parameters. The velocity scope of SMI was adapted to <2.5 cm/sec. Gentle pressure was applied through the transducer to prevent collapse of the vessels. Grey scale ultrasound the reactive nodes are hypoechoic, round to oval in shape. They show echogenic hilum with central hilar artery on color flow. On low flows dichomatous branching pattern is seen. Short axis to long axis ratio < 0.5. The nodes show low vascular resistance, low RI & PI. In inflammation due to vasodilatation increased blood flow in reactive lymph node, leading to low vascular resistance. Malignant nodes are usually hypoechoic, round shows no echogenic hilum. Eccentric cortical hypertrophy is suggestive of focal tumour infiltration. Cystic necrosis also suggestive of malignancy. A proven metastatic lymph node with ill defined borders may suggest extracapsular spread and patients may have a poor prognosis. Metastatic nodes from papillary carcinoma of the thyroid may be hyperechoic compared with adjacent muscles and have punctate calcifications.

In hodgkin's lymphoma and non hodgkin's lymphoma, lymph nodes tend to be round, hypoechoic and without echogenic hilum and tend to show intranodal reticulation. The differentiation of malignant from benign lymph nodes by ultrasound (US), computed tomography (CT) and magnetic resonance imaging (MRI) traditionally relies mainly on size measurements and topographic distribution [1-3]. However, sensitivity and specificity in the differentiation of benign and

malignant lymph nodes are disappointing using only size parameters. Reasons for the low accuracy include that malignant lymph node infiltration occurs in up to 30% in lymph nodes of less than 5 mm which has been shown for lung, esophageal, gastric, pancreatic and rectal carcinoma[4-10]. The evaluation of shape and border often adds no or only little more information to exclude malignancy[11,12]. New imaging methods should be able to delineate the early and circumscribed malignant infiltration and to improve ultrasound guided biopsy. Colour Doppler ultrasound (CDI) adds value for the differentiation of malignant from normal or reactive nodes by displaying the macrovessel architecture. Normal LNs generally show hilar predominant normal vascularity. Inflammatory lymph nodes are typically more vascularised without changes of the predominant hilar vessel architecture. In contrast metastatic lymph nodes present peripheral or mixed vascularity and loss of hilar type of vascularisation[13].

OBSERVATION AND RESULT

Table 1: Distribution of demographic and clinical data

Sr No	Study Variable	mesenteric lymphadenitis group N=77	control group N=84	Total	P Value
1	Age	12.23 ± 2.99	12.46 ± 3.12	12.3 ± 3.05	0.63
2	Gender				0.43
	a. Male	43 (27 %)	52 (32 %)	95 (59 %)	
	b. Female	34 (21 %)	32 (20 %)	66 (41 %)	
3	Symptoms				0.006
	a. Body Temperature (≥37.5°C)	62 (39 %)	51 (31 %)	113 (70 %)	0.09
	b. Nausea	61 (38 %)	58 (36 %)	119 (74 %)	0.14
	c. anorexia	47 (29 %)	42 (26 %)	89 (55 %)	0.16

Two hundred & fifty-three children were identified with Enlarged mesenteric lymph nodes and amongst these 166 met entry criteria; out of those 54 patients were operated or biopsied for confirmation of diagnosis. Mean age was 12.3 years (range 1.1–17.3 years). Enlarged mesenteric nodes were found in 253 in whom the largest enlarged mesenteric lymph node most frequently in the right lower quadrant (RIF) (222 of 253, 88%). Most of the children had three or more enlarged mesenteric nodes, all were in the RLQ. The largest short-axis diameter measured was 10 mm. 48 patients were associated with adjacent cecal thickening, appendicular pathology. Four were having matted, necrotic nodes, suspecting tuberculous pathology. Two were having round hypochoic nodes suspected to have lymphoma. These patients were operated or biopsied for confirmation of ultrasound findings. Histopathological correlation done to correlate ultrasound diagnosis in operated or biopsied patients to confirm ultrasound diagnosis.

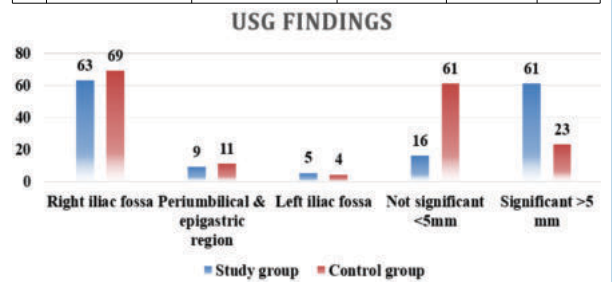
The definition of pathologic lymphadenopathy varies. Some studies suggest use of a longest diameter greater than 10 mm as pathologic, whereas some use the term mesenteric lymphadenitis only when the short axis diameter of the enlarged lymph node exceeds 10 mm. However, even small lymph nodes less than 5 mm in short axis diameter may be symptomatic. [20] Usually, 5 or more nodes are present and are often clustered. Nodal tenderness in response to transducer pressure is typical. Nodes are more rounded and hypochoic than normal. Abnormal nodes have a short-axis diameter of at least 5 mm, and the diameter can exceed 1 cm. The nodes are typically larger and more numerous with mesenteric lymphadenitis than with appendicitis (see the images below).

From the total number of patients five patients were excluded, due to technical problems in blood sampling (n=2) and incomplete ultrasound (US) imaging (n=3). Table 1 shows the

demographic and clinical data of the children included in the study. There was no significant difference in age or gender between the two groups (p>0.05). Body temperature of ≥37.5°C (70.4%), nausea (74.1%), and anorexia (55.6%) were the common clinical characteristics in children with mesenteric lymphadenitis.

Table 2: Distribution of USG findings

Sr No	USG Findings	mesenteric lymphadenitis group N=77	control group N=84	Total N=161	P Value
1	Site of nodes				0.86
	a. Right iliac fossa	63 (39 %)	69 (43 %)	132 (82 %)	
	b. Periumbilical & pigastric region	9 (6 %) 5 (3 %)	11 (6 %) 4 (3 %)	20 (12 %) 9 (6 %)	
	c. Left iliac fossa	.	.	.	
2	Size				<0.0001
	a. Not significant <5mm	16 (10 %)	61 (38 %)	77 (48 %)	
	b. Significant >5 mm	61 (38 %)	23 (14 %)	84 (52 %)	



Graph 1: Distribution of USG findings

In the mesenteric lymphadenitis group, there were 76.6% (59/77) enlarged mesenteric lymph nodes. In the control group, there were 72.6% (61/84) enlarged mesenteric lymph nodes. All the enlarged mesenteric lymph nodes in children were located in the right lower quadrant, whereas two were found in the left lower quadrant in one healthy child. Details of the mesenteric lymph nodes, including their size and shape, are shown in Table 2. The size of the mesenteric lymph nodes was greater in children with mesenteric lymphadenitis compared with the healthy control group. Both the greatest diameter and the least diameter of the mesenteric lymph nodes in children with mesenteric lymphadenitis was significantly greater than that of mesenteric lymph nodes in the normal healthy group (p<0.001). The mesenteric lymph nodes were mostly oval in shape in both groups (p=0.361).

Table 3: Distribution of blood flow findings

Sr No	Radiological modality	Number of cases N	Percentage %
1	Color Doppler flow imaging (CDFI)		
	Blood flow identification	137	85 %
	G1	71	44 %
	G2	47	29 %
2	Superb microvascular imaging (SMI)		
	Blood flow identification	148	92 %
	G2	89	55 %
	G3	35	22 %

There was a significant difference in the vascularity index between the two groups. Color Doppler flow imaging (CDFI) identified blood vessels in 85.2% (23/27) of the mesenteric lymph nodes in the mesenteric lymphadenitis group. Superb microvascular imaging (SMI) detected blood flow signals in

92.6% (25/27) of the mesenteric lymph nodes in the mesenteric lymphadenitis group (Table 3). In comparison, the majority of mesenteric lymph nodes in the control group showed no increase in vascularity using CDFI (83.3%) and SMI (80.0%) (Figure 1). CDFI showed that 74.0% of mesenteric lymph nodes were graded as G1 (44.4%) (Figure 2) and G2 (29.6%) in terms of the number of vessels visualized. SMI showed that 77.8% of mesenteric lymph nodes were graded as G2 (55.6%) and G3 (22.2%). These findings support that SMI was a superior imaging method for identifying both high-velocity and low-velocity blood flow.

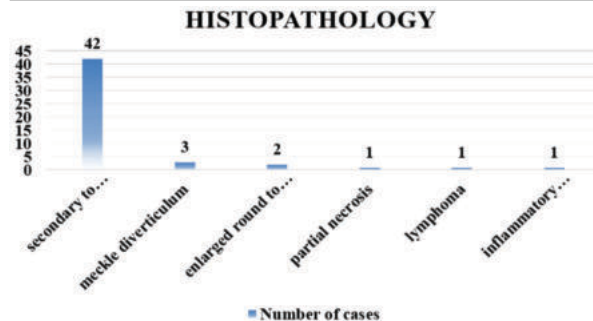
Out of 54 patient who were either operated or biopsied were confirmed on histopathology. 52 patients who had appendicular & tuberculous pathology on ultrasound/ CT 46 were turned to be secondary to appendicular inflammation. 3 were having associated meckle diverticulum. The two showed enlarged round to oblong shaped nodes with matting & one showed partial necrosis ,so were biopsied by transabdominal approach using 22 g trucut biopsy needle and were given as tuberculous turned out to be tuberculous etiology. Two patient in whom the nodes showed round hypoechoic appearance with edematous IC region, thought to inflammatory but biopsied, 1 turned out to be lymphoma one turned out to be inflammatory secondary to typhoid.

Table 4: Distribution of operated or biopsied cases on USG

Sr No	Associated Pathology	Number of cases N	Percentage %
1	adjacent cecal thickening, appendicular pathology	48	89 %
2	matted, necrotic nodes, suspecting tuberculous pathology	4	7 %
3	hypoechoic nodes suspected to have lymphoma	2	4 %
Total		54	100 %

Table 5: Distribution of operated or biopsied cases on histopathology

Sr No	Associated Pathology	Number of cases N	Percentage %
1	secondary to appendicular inflammation.	42	89 %
2	meckle diverticulum	3	7 %
3	enlarged round to oblong shaped nodes with matting	2	4 %
4	partial necrosis	1	2 %
5	lymphoma	1	2 %
6	inflammatory secondary to typhoid	1	2 %
Total		54	100 %

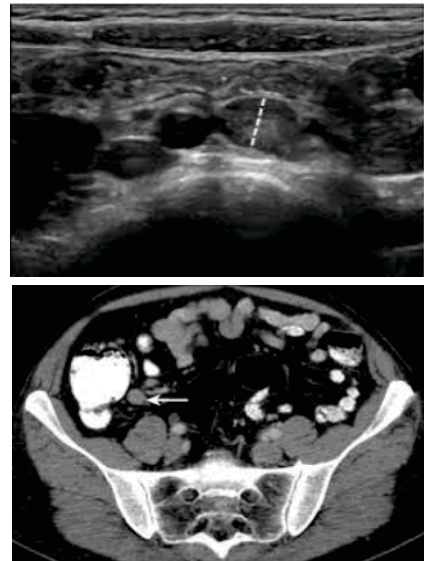


Graph 2: Distribution of operated or biopsied cases on histopathology

DISCUSSION

The inflammatory nodes are diagnosed by measuring transverse & long axis measurements with short axis

measurement of more than 8 mm. The nodes showed preserved central hilum, showed increased vascularity. There was no e/o necrosis or matting. The tuberculous nodes showed round to oval appearance with matting & few showed necrosis. The rounded hypoechoic nodes thought to be lymphoid origin, two turned out to be lymphoma, one turned out to be typhoid in etiology.



Summary

Mesenteric nodes with a short-axis diameter of >5–10 mm is commonly found on abdominal Ultrasound or CT examination of children with a low likelihood for mesenteric lymphadenopathy and should be considered a non-specific finding. A short-axis diameter of 8 mm might better define the upper limit of normal mesenteric lymph node size in children. The differentiation of malignant from benign lymph nodes by ultrasound (US), computed tomography (CT) and magnetic resonance imaging (MRI) traditionally relies mainly on size measurements and topographic distribution[1-3]. However, sensitivity and specificity in the differentiation of benign and malignant lymph nodes are disappointing using only size parameters. Reasons for the low accuracy include that malignant lymph node infiltration occurs in up to 30% in lymph nodes of less than 5 mm which has been shown for lung, esophageal, gastric, pancreatic and rectal carcinoma[4-10]. The evaluation of shape and border often adds no or only little more information to exclude malignancy[11,12]. New imaging methods should be able to delineate the early and circumscribed malignant infiltration and to improve ultrasound guided biopsy. Colour Doppler ultrasound (CDI) adds value for the differentiation of malignant from normal or reactive nodes by displaying the macrovessel architecture. Normal LNs generally show hilar predominant normal vascularity. Inflammatory lymph nodes are typically more vascularised without changes of the predominant hilar vessel architecture. In contrast metastatic lymph nodes present peripheral or mixed vascularity and loss of hilar type of vascularisation[13]. The differentiation of malignant from benign lymph nodes by ultrasound (US), computed tomography (CT) and magnetic resonance imaging (MRI) traditionally relies mainly on size measurements and topographic distribution[1-3]. However, sensitivity and specificity in the differentiation of benign and malignant lymph nodes are disappointing using only size parameters. Reasons for the low accuracy include that malignant lymph node infiltration occurs in up to 30% in lymph nodes of less than 5 mm which has been shown for lung, esophageal, gastric, pancreatic and rectal carcinoma[4-10]. The evaluation of shape and border often adds no or only little more information to exclude malignancy[11,12]. New imaging methods should be able to delineate the early and

circumscribed malignant infiltration and to improve ultrasound guided biopsy. Colour Doppler ultrasound (CDI) adds value for the differentiation of malignant from normal or reactive nodes by displaying the macrovessel architecture. Normal LNs generally show hilar predominant normal vascularity. Inflammatory lymph nodes are typically more vascularised without changes of the predominant hilar vessel architecture. In contrast metastatic lymph nodes present peripheral or mixed vascularity and loss of hilar type of vascularisation[13].

REFERENCES

1. Sharma A, Fidias P, Hayman LA, Loomis SL, Taber KH, Aquino SL. Patterns of lymphadenopathy in thoracic malignancies. *Radiographics*. 2004;24: 419-434.
2. Sumi M, Ohki M, Nakamura T. Comparison of sonography and CT for differentiating benign from malignant cervical lymph nodes in patients with squamous cell carcinoma of the head and neck. *AJR Am J Roentgenol*. 2001;176:1019-1024.
3. Hocke M, Menges M, Topalidis T, Dietrich CF, Stallmach A. Contrast-enhanced endoscopic ultrasound in discrimination between benign and malignant mediastinal and abdominal lymph nodes. *J Cancer Res Clin Oncol*. 2008;134:473-480.
4. Prenzel KL, Höltscher AH, Drebber U, Agavonova M, Gutschow CA, Bollschweiler E. Prognostic impact of nodal micrometastasis in early esophageal cancer. *Eur J Surg Oncol*. 2012;38:314-318.
5. Prenzel KL, Mönig SP, Sinning JM, Baldus SE, Brochhagen HG, Schneider PM, Höltscher AH. Lymph node size and metastatic infiltration in non-small cell lung cancer. *Chest*. 2003;123:463-467.
6. Prenzel KL, Höltscher AH, Vallböhrner D, Drebber U, Gutschow CA, Mönig SP, Stippel DL. Lymph node size and metastatic infiltration in adenocarcinoma of the pancreatic head. *Eur J Surg Oncol*. 2010;36:993-996.
7. Janssen C, Dietrich CF, Burmester E. [Malignant neoplasias of the gastrointestinal tract--endoscopic ultrasonic staging revisited]. *Z Gastroenterol*. 2011;49:357-368.
8. Moehler M, Al-Batran SE, Andrus T, Anthuber M, Arends J, Arnold D, Aust D, Baier P, Baretton G, Bernhardt J, et al. German S3-guideline "Diagnosis and treatment of esophagogastric cancer." *Z Gastroenterol*. 2011;49:461-531.
9. Jürgensen C, Dietrich CF. Role of endoscopic ultrasound (EUS) in the staging of rectal cancer. *Z Gastroenterol*. 2008;46:580-589.
10. Janssen C, Dietrich CF. Endoscopic ultrasound-guided fine-needle aspiration biopsy and trucut biopsy in gastroenterology - An overview. *Best Pract Res Clin Gastroenterol*. 2009;23:743-759.
11. Ying M, Ahuja A, Brook F, Brown B, Metreweli C. Nodal shape (S/L) and its combination with size for assessment of cervical lymphadenopathy: which cut-off should be used. *Ultrasound Med Biol*. 1999;25:1169-1175.
12. Vassallo P, Wernecke K, Roos N, Peters PE. Differentiation of benign from malignant superficial lymphadenopathy: the role of high-resolution US. *Radiology*. 1992;183:215-220.
13. Ahuja AT, Ying M. Sonographic evaluation of cervical lymph nodes. *AJR Am J Roentgenol*. 2005;184:1691-1699.
14. Schmid-Wendtner MH, Partsch K, Korting HC, Volkenandt M. Improved differentiation of benign and malignant lymphadenopathy in patients with cutaneous melanoma by contrast-enhanced color Doppler sonography. *Arch Dermatol*. 2002;138:491-497.
15. Hocke M, Schulze E, Gottschalk P, Topalidis T, Dietrich CF. Contrast-enhanced endoscopic ultrasound in discrimination between focal pancreatitis and pancreatic cancer. *World J Gastroenterol*. 2006;12:246-250.
16. Ying M, Ahuja A. Sonography of neck lymph nodes. Part I: normal lymph nodes. *Clin Radiol*. 2003;58:351-358.
17. Ahuja A, Ying M. Sonographic evaluation of cervical lymphadenopathy: is power Doppler sonography routinely indicated. *Ultrasound Med Biol*. 2003;29:353-359.
18. Tschammler A, Heuser B, Ott G, Schmitt S, Hahn D. Pathological angioarchitecture in lymph nodes: underlying histopathologic findings. *Ultrasound Med Biol*. 2000;26:1089-1097.
19. Moritz JD, Ludwig A, Oestmann JW. Contrast-enhanced color Doppler sonography for evaluation of enlarged cervical lymph nodes in head and neck tumors. *AJR Am J Roentgenol*. 2000;174:1279-1284.
20. Claudon M, Dietrich CF, Choi BI, Cosgrove DO, Kudo M, Nolsoe CP, Piscaglia F, Wilson SR, Barr RG, Chammas MC, et al. Guidelines and good clinical practice recommendations for contrast enhanced ultrasound (CEUS) in the liver - update 2012: a WFUMB-EFSUMB initiative in cooperation with representatives of AFSUMB, AIUM, ASUM, FLAUS and ICUS. *Ultraschall Med*. 2013;34:11-29.
21. Claudon M, Dietrich CF, Choi BI, Cosgrove DO, Kudo M, Nolsoe CP, Piscaglia F, Wilson SR, Barr RG, Chammas MC, et al. Guidelines and good clinical practice recommendations for Contrast Enhanced Ultrasound (CEUS) in the liver - update 2012: A WFUMB-EFSUMB initiative in cooperation with representatives of AFSUMB, AIUM, ASUM, FLAUS and ICUS. *Ultrasound Med Biol*. 2013;39:187-210.
22. Piscaglia F, Nolsoe C, Dietrich CF, Cosgrove DO, Gilja OH, Bachmann Nielsen M, Albrecht T, Barozzi L, Bertolotto M, Catalano O, et al. The EFSUMB Guidelines and Recommendations on the Clinical Practice of Contrast Enhanced Ultrasound (CEUS): update 2011 on non-hepatic applications. *Ultraschall Med*. 2012;33:33-59.
23. Rubaltelli L, Khadivi Y, Tregnaghi A, Stramare R, Ferro F, Borsato S, Fiocco U, Adami F, Rossi CR. Evaluation of lymph node perfusion using continuous mode harmonic ultrasonography with a second-generation contrast agent. *J Ultrasound Med*. 2004;23:829-836.
24. Rubaltelli L, Beltrame V, Tregnaghi A, Scagliori E, Frigo AC, Stramare R. Contrast-enhanced ultrasound for characterizing lymph nodes with focal cortical thickening in patients with cutaneous melanoma. *AJR Am J Roentgenol*. 2011;196:W8-12.

25. Yu M, Liu Q, Song HP, Han ZH, Su HL, He GB, Zhou XD. Clinical application of contrast-enhanced ultrasonography in diagnosis of superficial lymphadenopathy. *J Ultrasound Med*. 2010;29:735-740.
26. Ouyang Q, Chen L, Zhao H, Xu R, Lin Q. Detecting metastasis of lymph nodes and predicting aggressiveness in patients with breast carcinomas. *J Ultrasound Med*. 2010;29:343-352.
27. Wan CF, Du J, Fang H, Li FH, Zhu JS, Liu Q. Enhancement patterns and parameters of breast cancers at contrast-enhanced US: correlation with prognostic factors. *Radiology*. 2012;262:450-459.
28. Yang WT, Metreweli C, Lam PK, Chang J. Benign and malignant breast masses and axillary nodes: evaluation with echo-enhanced color power Doppler US. *Radiology*. 2001;220:795-802.
29. Sakaguchi T, Yamashita Y, Katahira K, Nishimura R, Baba Y, Arakawa A, Takahashi M, Yumoto E, Shinohara M. Differential diagnosis of small round cervical lymph nodes: comparison of power Doppler US with contrast-enhanced CT and pathologic results. *Radiat Med*. 2001;19:119-125.
30. King AD, Tse GM, Ahuja AT, Yuen EH, Vliantis AC, To EW, van Hasselt AC. Necrosis in metastatic neck nodes: diagnostic accuracy of CT, MR imaging, and US. *Radiology*. 2004;230:720-726.
31. Nakase K, Yamamoto K, Hiasa A, Tawara I, Yamaguchi M, Shiku H. Contrast-enhanced ultrasound examination of lymph nodes in different types of lymphoma. *Cancer Detect Prev*. 2006;30:188-191.
32. Berho M, Oviedo M, Stone E, Chen C, Nogueras J, Weiss E, Sands D, Wexner S. The correlation between tumour regression grade and lymph node status after chemoradiation in rectal cancer. *Colorectal Dis*. 2009;11:254-258.
33. Ahuja AT, Ying M, Ho SY, Antonio G, Lee YP, King AD, Wong KT. Ultrasound of malignant cervical lymph nodes. *Cancer Imaging*. 2008;8:48-56.
34. Eich HT, Müller RP, Engenhardt-Cabillic R, Lukas P, Schmidberger H, Staar S, Willich N. Involved-node radiotherapy in early-stage Hodgkin's lymphoma. Definition and guidelines of the German Hodgkin Study Group (GHSG) *Strahlenther Onkol*. 2008;184:406-410.
35. Engert A, Eichenauer DA, Dreyling M. Hodgkin's lymphoma: ESMO clinical recommendations for diagnosis, treatment and follow-up. *Ann Oncol*. 2009;20 Suppl 4:108-109.
36. Ignee A, Jedrejczyk M, Schuessler G, Jakubowski W, Dietrich CF. Quantitative contrast enhanced ultrasound of the liver for time intensity curves-Reliability and potential sources of errors. *Eur J Radiol*. 2010;73:153-158.
37. Rubaltelli L, Corradin S, Dorigo A, Tregnaghi A, Adami F, Rossi CR, Stramare R. Automated quantitative evaluation of lymph node perfusion on contrast-enhanced sonography. *AJR Am J Roentgenol*. 2007;188:977-983.
38. Steppan I, Reimer D, Müller-Holzner E, Marth C, Aigner F, Frauscher F, Frede T, Zeimet AG. Breast cancer in women: evaluation of benign and malignant axillary lymph nodes with contrast-enhanced ultrasound. *Ultraschall Med*. 2010;31:63-67.
39. Dietrich CF, Averkiou MA, Correias JM, Lassau N, Leen E, Piscaglia F. An EFSUMB introduction into Dynamic Contrast-Enhanced Ultrasound (DCE-US) for quantification of tumour perfusion. *Ultraschall Med*. 2012;33:344-351.
40. Dietrich CF. Elastography, the new dimension in ultrasonography. *Praxis (Bern 1994)* 2011;100:1533-1542.
41. Sftou A, Vilmann P, Hassan H, Gorunescu F. Analysis of endoscopic ultrasound elastography used for characterisation and differentiation of benign and malignant lymph nodes. *Ultraschall Med*. 2006;27:535-542.
42. Janssen J. [(E)US elastography: current status and perspectives] *Z Gastroenterol*. 2008;46:572-579.
43. Giovannini M, Thomas B, Erwan B, Christian P, Fabrice C, Benjamin E, Geneviève M, Paolo A, Pierre D, Robert Y, et al. Endoscopic ultrasound elastography for evaluation of lymph nodes and pancreatic masses: a multicenter study. *World J Gastroenterol*. 2009;15:1587-1593.
44. Dietrich CF. *Elastography Applications*. Endo heute. 2011;24:177-212.
45. Larsen MH, Frstrup C, Hansen TP, Hovendal CP, Mortensen MB. Endoscopic ultrasound, endoscopic sonoelastography, and strain ratio evaluation of lymph nodes with histology as gold standard. *Endoscopy*. 2012;44:759-766.
46. Bachmann-Nielsen M, Sftou A. [Elastography - true or false. *Ultraschall Med*. 2011;32:5-7.
47. Sftou A, Vilmann P, Ciurea T, Popescu GL, Iordache A, Hassan H, Gorunescu F, Iordache S. Dynamic analysis of EUS used for the differentiation of benign and malignant lymph nodes. *Gastrointest Endosc*. 2007;66:291-300.
48. Wojcinski S, Dupont J, Schmidt W, Cassel M, Hillemanns P. Real-time ultrasound elastography in 180 axillary lymph nodes: elasticity distribution in healthy lymph nodes and prediction of breast cancer metastases. *BMC Med Imaging*. 2012;12:35.
49. Wing-Han Yuen Q, Zheng YP, Huang YP, He JF, Chung-Wai Cheung J, Ying M. In-vitro Strain and Modulus Measurements in Porcine Cervical Lymph Nodes. *Open Biomed Eng J*. 2011;5:39-46.
50. Bamber J, C1 Bamber J, Cosgrove D, Dietrich CF, Fromageau J, Bojunga J, Calliada F, Cantisani V, Correias JM, D'Onofrio M, et al. EFSUMB guidelines and recommendations on the clinical use of ultrasound elastography. Part 1: Basic principles and technology. *Ultraschall Med*. 2013;34:169-184.
51. Cosgrove D, Piscaglia F, Bamber J, Bojunga J, Correias JM, Gilja OH, Klausner AS, Sporea I, Calliada F, Cantisani V, et al. EFSUMB guidelines and recommendations on the clinical use of ultrasound elastography. Part 2: Clinical applications. *Ultraschall Med*. 2013;34:238-253.
52. Lyshchik A, Higashi T, Asato R, Tanaka S, Ito J, Hiraoka M, Insana MF, Brill AB, Saga T, Togashi K. Cervical lymph node metastases: diagnosis at sonoelastography--initial experience. *Radiology*. 2007;243:258-267.
53. Tan R, Xiao Y, He Q. Ultrasound elastography: Its potential role in assessment of cervical lymphadenopathy. *Acad Radiol*. 2010;17:849-855.
54. Teng DK, Wang H, Lin YQ, Sui GQ, Guo F, Sun LN. Value of ultrasound elastography in assessment of enlarged cervical lymph nodes. *Asian Pac J Cancer Prev*. 2012;13:2081-2085.
55. Ishibashi N, Yamagata K, Sasaki H, Seto K, Shinya Y, Ito H, Shinozuka K, Yanagawa T, Onizawa K, Bukawa H. Real-time tissue elastography for the diagnosis of lymph node metastasis in oral squamous cell carcinoma. *Ultrasound Med Biol*. 2012;38:389-395.
56. Choi JJ, Kang BJ, Kim SH, Lee JH, Jeong SH, Yim HW, Song BJ, Jung SS. Role of sonographic elastography in the differential diagnosis of axillary lymph nodes in breast cancer. *J Ultrasound Med*. 2011;30:429-436.
57. Taylor K, O'Keefe S, Britton PD, Wallis MG, Treece GM, Housden J, Parashar D.

- Bond S, Sinnatamby R. Ultrasound elastography as an adjuvant to conventional ultrasound in the preoperative assessment of axillary lymph nodes in suspected breast cancer: a pilot study. *Clin Radiol.* 2011; 66:1064–1071.
58. Bhatia KS, Cho CC, Tong CS, Yuen EH, Ahuja AT. Shear wave elasticity imaging of cervical lymph nodes. *Ultrasound Med Biol.* 2012;38:195–201.
59. Bhatia K, Tong CS, Cho CC, Yuen EH, Lee J, Ahuja AT. Reliability of shear wave ultrasound elastography for neck lesions identified in routine clinical practice. *Ultraschall Med.* 2012;33:463–468.
60. Ying L, Hou Y, Zheng HM, Lin X, Xie ZL, Hu YP. Real-time elastography for the differentiation of benign and malignant superficial lymph nodes: a meta-analysis. *Eur J Radiol.* 2012;81:2576–2584.
61. Dietrich CF, Janssen C. Evidence based endoscopic ultrasound. *Z Gastroenterol.* 2011;49:599–621.
62. Dietrich CF, Hocke M, Janssen C. Interventional endosonography. *Ultraschall Med.* 2011;32:8–22, quiz 23–25.
63. Dietrich CF. Contrast-enhanced low mechanical index endoscopic ultrasound (CELMi-EUS) Endoscopy. 2009;41 Suppl 2:E43–E44.
64. Kanamori A, Hirooka Y, Itoh A, Hashimoto S, Kawashima H, Hara K, Uchida H, Goto J, Ohmiya N, Niwa Y, et al. Usefulness of contrast-enhanced endoscopic ultrasonography in the differentiation between malignant and benign lymphadenopathy. *Am J Gastroenterol.* 2006;101:45–51.
65. Sakamoto H, Kitano M, Matsui S, Kamata K, Komaki T, Imai H, Dote K, Kudo M. Estimation of malignant potential of GI stromal tumors by contrast-enhanced harmonic EUS (with videos) *GastrointestEndosc.* 2011;73:227–237.
66. Kannengiesser K, Mahlke R, Petersen F, Peters A, Ross M, Kucharzik T, Maaser C. Contrast-enhanced harmonic endoscopic ultrasound is able to discriminate benign submucosal lesions from gastrointestinal stromal tumors. *Scand J Gastroenterol.* 2012;47:1515–1520.
67. Dietrich CF, Janssen C, Hocke M, Cui XW, Woenckhaus M, Ignee A. Imaging of gastrointestinal stromal tumours with modern ultrasound techniques - a pictorial essay. *Z Gastroenterol.* 2012;50:457–467.
68. Gong TT, Hu DM, Zhu Q. Contrast-enhanced EUS for differential diagnosis of pancreatic mass lesions: a meta-analysis. *GastrointestEndosc.* 2012; 76: 301–309.
69. Napoleon B, Alvarez-Sanchez MV, Gincoul R, Pujol B, Lefort C, Lepilliez V, Labadie M, Souquet JC, Queneau PE, Scoazec JY, et al. Contrast-enhanced harmonic endoscopic ultrasound in solid lesions of the pancreas: results of a pilot study. *Endoscopy.* 2010;42:564–570.
70. Kitano M, Kudo M, Yamao K, Takagi T, Sakamoto H, Komaki T, Kamata K, Imai H, Chiba Y, Okada M, et al. Characterization of small solid tumors in the pancreas: the value of contrast-enhanced harmonic endoscopic ultrasonography. *Am J Gastroenterol.* 2012;107:303–310.
71. Reddy NK, Ioncic AM, Sftiou A, Vilmann P, Bhutani MS. Contrast-enhanced endoscopic ultrasonography. *World J Gastroenterol.* 2011;17:42–48.
72. Sftiou A, Vilmann P, Gorunescu F, Janssen J, Hocke M, Larsen M, Iglesias-Garcia J, Arcidiacono P, Will U, Giovannini M, et al. Accuracy of endoscopic ultrasound elastography used for differential diagnosis of focal pancreatic masses: a multicenter study. *Endoscopy.* 2011;43:596–603.
73. Sftiou A, Dietrich CF, Vilmann P. Contrast-enhanced harmonic endoscopic ultrasound. *Endoscopy.* 2012;44:612–617.
74. Hocke M, Ignee A, Topalidis T, Stallmach A, Dietrich CF. Contrast-enhanced endosonographic Doppler spectrum analysis is helpful in discrimination between focal chronic pancreatitis and pancreatic cancer. *Pancreas.* 2007;35:286–288.
75. Dietrich CF, Ignee A, Braden B, Barreiros AP, Ott M, Hocke M. Improved differentiation of pancreatic tumors using contrast-enhanced endoscopic ultrasound. *Clin Gastroenterol Hepatol.* 2008;6:590–597.e1.
76. Park CH, Chung MJ, Oh TG, Park JY, Bang S, Park SW, Kim H, Hwang HK, Lee WJ, Song SY. Differential diagnosis between gallbladder adenomas and cholesterol polyps on contrast-enhanced harmonic endoscopic ultrasonography. *Surg Endosc.* 2013;27:1414–1421.
77. Romagnuolo J, Hoffman B, Vela S, Hawes R, Vignesh S. Accuracy of contrast-enhanced harmonic EUS with a second-generation perflutren lipid microsphere contrast agent (with video) *GastrointestEndosc.* 2011;73:52–63.
78. Xia Y, Kitano M, Kudo M, Imai H, Kamata K, Sakamoto H, Komaki T. Characterization of intra-abdominal lesions of undetermined origin by contrast-enhanced harmonic EUS (with videos) *GastrointestEndosc.* 2010;72:637–642.
79. Janssen J, Dietrich CF, Will U, Greiner L. Endosonographic elastography in the diagnosis of mediastinal lymph nodes. *Endoscopy.* 2007;39:952–957.
80. Larsen MH, Frstrup CW, Mortensen MB. Intra- and interobserver agreement of endoscopic sonoelastography in the evaluation of lymph nodes. *Ultraschall Med.* 2011;32 Suppl 2:E45–E50.
81. Paterson S, Duthie F, Stanley AJ. Endoscopic ultrasound-guided elastography in the nodal staging of oesophageal cancer. *World J Gastroenterol.* 2012;18:889–895.
82. Knabe M, Günter E, Ell C, Pech O. Can EUS elastography improve lymph node staging in esophageal cancer. *Surg Endosc.* 2013;27:1196–1202.
83. Xu W, Shi J, Zeng X, Li X, Xie WF, Guo J, Lin Y. EUS elastography for the differentiation of benign and malignant lymph nodes: a meta-analysis. *GastrointestEndosc.* 2011;74:1001–1009;quiz 1115.e1-4.
84. Omoto K, Matsunaga H, Take N, Hozumi Y, Takehara M, Omoto Y, Shiozawa M, Mizunuma H, Harashima H, Taniguchi N, et al. Sentinel node detection method using contrast-enhanced ultrasonography with sonazoid in breast cancer: preliminary clinical study. *Ultrasound Med Biol.* 2009;35:1249–1256.
85. De Giorgi V, Gori A, Crazzini M, Rossari S, Marino G, D'Elia G, Crocetti E, Roselli G, Innocenti P, Dini M, et al. Contrast-enhanced ultrasound: a filter role in AJCC stage I/II melanoma patients. *Oncology.* 2010;79:370–375.
86. Sever A, Jones S, Cox K, Weeks J, Mills P, Jones P. Preoperative localization of sentinel lymph nodes using intradermal microbubbles and contrast-enhanced ultrasonography in patients with breast cancer. *Br J Surg.* 2009;96:1295–1299.
87. Sever AR, Mills P, Weeks J, Jones SE, Fish D, Jones PA, Mali W. Preoperative needle biopsy of sentinel lymph nodes using intradermal microbubbles and contrast-enhanced ultrasound in patients with breast cancer. *AJR Am J Roentgenol.* 2012;199:465–470.
88. Sever AR, Mills P, Jones SE, Mali W, Jones PA. Sentinel node identification using microbubbles and contrast-enhanced ultrasonography. *Clin Radiol.* 2012;67:687–694.
89. Sever AR, Mills P, Jones SE, Cox K, Weeks J, Fish D, Jones PA. Preoperative sentinel node identification with ultrasound using microbubbles in patients with breast cancer. *AJR Am J Roentgenol.* 2011;196:251–256.
90. Cui XW, Ignee A, Nielsen MB, Schreiber-Dietrich D, De Molo C, Pirri C, Jedrzejczyk M, Dietrich CF. Contrast enhanced ultrasound of sentinel lymph nodes. *J Ultrason.* 2013;13:73–81.
91. Bialek EJ, Jakubowski W, Szczepanik AB, Maryniak RK, Bilski R, Prochorec-Sobieszek M, Serafin-Krol M. 3D ultrasound examination of the superficial lymph nodes—does it provide additional information. *Ultraschall Med.* 2006;27:467–472.
92. Dietrich CF. 3D real time contrast enhanced ultrasonography, a new technique. *Rofo.* 2002;174:160–163.
93. Hocke M, Dietrich CF. New technology—combined use of 3D contrast enhanced endoscopic ultrasound techniques. *Ultraschall Med.* 2011; 32:317–318.